Physica E 86 (2017) 146–153

Contents lists available at ScienceDirect

Physica E

journal homepage: www.elsevier.com/locate/physe

The effects of different nano particles of Al_2O_3 and Ag on the MHD nano fluid flow and heat transfer in a microchannel including slip velocity and temperature jump

Arash Karimipour[a,*], Annunziata D'Orazio[b], Mostafa Safdari Shadloo[c]

[a] Department of Mechanical Engineering, Najafabad Branch, Islamic Azad University, Najafabad, Iran
[b] Dipartimento di Ingegneria Astronautica, Elettrica ed Energetica, Facoltà di Ingegneria, Sapienza Università di Roma, Via Eudossiana, 18-00184 Rome, Italy
[c] CORIA-UMR 6614, Normandie University, CNRS-University & INSA of Rouen, 76000 Rouen, France

ARTICLE INFO

Keywords:
Nano particles
Nano fluid
Slip flow
Magneto hydro dynamic

ABSTRACT

The forced convection of nanofluid flow in a long microchannel is studied numerically according to the finite volume approach and by using a developed computer code. Microchannel domain is under the influence of a magnetic field with uniform strength. The hot inlet nanofluid is cooled by the heat exchange with the cold microchannel walls. Different types of nanoparticles such as Al_2O_3 and Ag are examined while the base fluid is considered as water. Reynolds number are chosen as Re=10 and Re=100. Slip velocity and temperature jump boundary conditions are simulated along the microchannel walls at different values of slip coefficient for different amounts of Hartmann number. The investigation of magnetic field effect on slip velocity and temperature jump of nanofluid is presented for the first time. The results are shown as streamlines and isotherms; moreover the profiles of slip velocity and temperature jump are drawn. It is observed that more slip coefficient corresponds to less Nusselt number and more slip velocity especially at larger Hartmann number. It is recommended to use Al_2O_3-water nanofluid instead of Ag-water to increase the heat transfer rate from the microchannel walls at low values of Re. However at larger amounts of Re, the nanofluid composed of nanoparticles with higher thermal conductivity works better.

1. Introduction

Due to low thermal conductivity of liquids, the main heat transfer mechanism is considered as the convection among them. Hence the enhancement of liquid thermal conductivity can invigorate the total heat transfer rate from. In this way, using nanofluid can be useful which is a mixture of solid nanoparticles suspended in the base fluid. Higher thermal conductivity of nanoparticles corresponds to more thermal conductivity of the mixture and increases the conduction heat transfer beside its convection [1–6].

Several works can be referred which used nanofluid at different physical conditions such as the forced and natural convection in the enclosures or the nanofluid flow through the pipes and ducts. However, using nanofluid in heat exchangers or in the more complex geometries is also reported in some other articles [7–12]. Among them Oztop and Abu-Nada [13] reported the natural convection of nanofluid in partially heated rectangular enclosure for different kinds of nanoparticles such as TiO_2, Cu, AL_2O_3. Moreover the enhancement of Nusselt number of Cu-water nanofluid in a lid-driven cavity was observed in those of Tiwari and Das [14]. A large number of articles can be addressed which studied the mixed convection of nanofluids filled in the closed or open cavities [15–21]. Applying the nanofluid is not limited to the laminar single phase flows; hence a great number of works tried to investigate the nanofluid flow in turbulent regime or supposing it as a two-phase mixture [22–24].

The fluid flow and heat transfer at micro-scales level are completely different from the macro-scales one. More efficiency beside the small size of a micro-device encourages researchers to pay more attention on [25–29]. The gas micro-flows are classified according to the Knudsen number while at $Kn < 0.001$, the flow regime is continuum and could be simulated by classic Navier-Stokes equations. However at $0.001 < Kn < 0.1$, the slip flow regime is dominated and Navier-Stokes equations with the slip boundary condition must be used [30–34]. Moreover at $0.1 < Kn < 10$ and $Kn > 10$, the transient and free molecular regimes are treated the flow, respectively and the particle base methods should be applied [35–42].

* Corresponding author.
E-mail addresses: arashkarimipour@gmail.com (A. Karimipour), annunziata.dorazio@uniroma1.it (A. D'Orazio), msshadloo@coria.fr (M.S. Shadloo).

http://dx.doi.org/10.1016/j.physe.2016.10.015
Received 9 July 2016; Received in revised form 28 September 2016; Accepted 9 October 2016
Available online 13 October 2016
1386-9477/

Nomenclature

AR	aspect ratio of the microchannel (=L/H)
B	slip coefficient in non-dimensional form (=β/h)
B_0	the strength of magnetic field
c_p	diameter of nanoparticles (=10 nm)
d_p	diameter of nanoparticles (=10 nm)
h	the height of Microchannel (m)
H	the height of Microchannel in non-dimensional form
Ha	Hartmann number
k	thermal conductivity (W m^{-1} K^{-1})
l	the length of microchannel (m)
L	the length of microchannel in non-dimensional form
Nu	Nusselt number
p	pressure (Pa)
P	pressure in non-dimensional form
Pr	Prandtl number
Re	Reynolds number
T	temperature (K)
T_C	the temperature of cold walls (K)
T_H	the temperature of hot inlet nanofluid (K)
u	horizontal velocity (m s^{-1})
u_i	inlet velocity (m s^{-1})
U	horizontal velocity in non-dimensional form
U_s	slip velocity in non-dimensional form
v	vertical velocity (m s^{-1})
V	vertical velocity in non-dimensional form
x	horizontal Cartesian coordinate (m)
X	horizontal Cartesian coordinate in non-dimensional form
y	vertical Cartesian coordinate (m)
Y	vertical Cartesian coordinate in non-dimensional form

Greek symbols

α	thermal diffusivity (m^2 s^{-1})
β	slip coefficient (m)
σ	electrical conductivity (S m^{-1})
φ	volume fraction of nanoparticles
μ	dynamic viscosity (N sm^{-2})
θ	temperature in non-dimensional form
θ_s	temperature jump in non-dimensional form
ρ	density (kg m^{-3})
υ	kinematic viscosity (m^2 s^{-1})

Subscripts

f	fluid
nf	nanofluid
s	solid nanoparticles

For a liquid micro-flow at slip flow regime (like the nanofluid flow through a microchannel), the slip coefficient is defined as β (and not as Kn) and the no-slip boundary condition is dropped; so that the slip velocity and temperature jump boundary conditions should be involved. The combination of a nanofluid flow in a microchannel might be an innovative way to enhance the heat transfer rate at micro scales level [43–47]. The investigation of the magneto-hydrodynamic field effect (MHD) on hydrodynamic and thermal properties of a fluid flow was presented as a follow-up case study; which implies the flow of electrically conducting fluid in a duct happens in the presence of a transverse magnetic field and generates the Lorentz force against the fluid flow direction [48–53].

Present work aims to simulate the nanofluid flow in a microchannel in the presence of a magnetic field. However what distinguishes this study from the previous articles is the investigation of magnetic field effects on nanofluid slip velocity and temperature jump for the first time (to the best of authors' knowledge) which was ignored in previous papers [54].

2. Problem statement

The forced convection of Newtonian homogeneous nanofluid flow in a long microchannel with aspect ratio of AR=L/H=30, is studied numerically. Microchannel domain is under the influence of a magnetic field with strength of B_0 as shown in Fig. 1. The hot inlet nanofluid is cooled by the heat exchange with the cold microchannel walls. Different types of nanoparticles such as Al_2O_3 and Ag are examined at fixed value of nanoparticles volume fraction (φ=0.04=4%), while the base fluid is considered as water. The nanoparticles diameter are supposed as d_p=10 nm.

Duo to represent a real physical situation, Nanofluid Reynolds number (*Re*) could not be a large value through the microchannel; so that Reynolds number are chosen as *Re*=10 and *Re*=100. Slip velocity and temperature jump boundary conditions are simulated along the microchannel walls at different values of slip coefficient (B=0.01, B=0.05 and B=0.1) for different amounts of Hartmann number (*Ha*=0, *Ha*=20 and *Ha*=40). As a result, the investigation of magnetic field effect on slip velocity and temperature jump of nanofluid flow through the microchannel is presented for the first time at present article.

3. Formulation

Two-dimensional Navier-Stokes equations are applied for the nanofluid flow considering magnetic field effect as [55]:

Continuity equation:

$$\frac{\partial u}{\partial x}+\frac{\partial v}{\partial y}=0 \tag{1}$$

Momentum equation along the x-coordinates:

$$u\frac{\partial u}{\partial x}+v\frac{\partial u}{\partial y}=-\frac{1}{\rho_{nf}}\frac{\partial p}{\partial x}+\upsilon_{nf}\left(\frac{\partial^2 u}{\partial x^2}+\frac{\partial^2 u}{\partial y^2}\right)-\frac{\sigma_{nf}B_0^2}{\rho_{nf}}u \tag{2}$$

Momentum equation along the y-coordinates:

$$u\frac{\partial v}{\partial x}+v\frac{\partial v}{\partial y}=-\frac{1}{\rho_{nf}}\frac{\partial p}{\partial y}+\upsilon_{nf}\left(\frac{\partial^2 v}{\partial x^2}+\frac{\partial^2 v}{\partial y^2}\right) \tag{3}$$

Energy equation:

$$u\frac{\partial T}{\partial x}+v\frac{\partial T}{\partial y}=\alpha_{nf}\left(\frac{\partial^2 T}{\partial x^2}+\frac{\partial^2 T}{\partial y^2}\right) \tag{4}$$

Density and viscosity of the nanofluid can be estimated by Eqs. (5) and (6) using nanoparticles volume fraction; while the subscripts f, s and nf represent the base-fluid, solid nanoparticles and nanofluid, respectively:

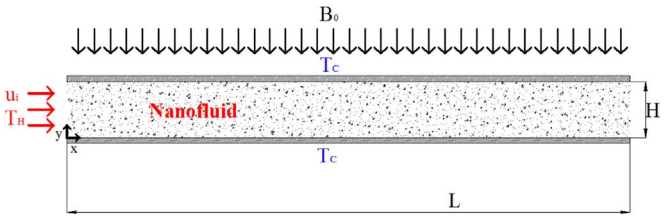

Fig. 1. Physical domain of microchannel.

Table 1
Thermo-physical properties of nano particles and water.

	c_p (J/kg K)	ρ (kg m^{-3})	K (W/mK)	μ (Pa s)
Water	4179	997	0.6	8.91×10^{-4}
Ag	235	10,500	429	–
Al_2O_3	765	3970	40	–

Table 2
Grid independency study for the values of U and θ at X=L/2 and Y=H/2 for φ=0.04, *Re*=10, *Ha*=0 and B=0.1 for water-Al_2O_3 nanofluid.

	375×25	450×30	525×35
U	1.309	1.310	1.310
θ	0.131	0.133	0.134

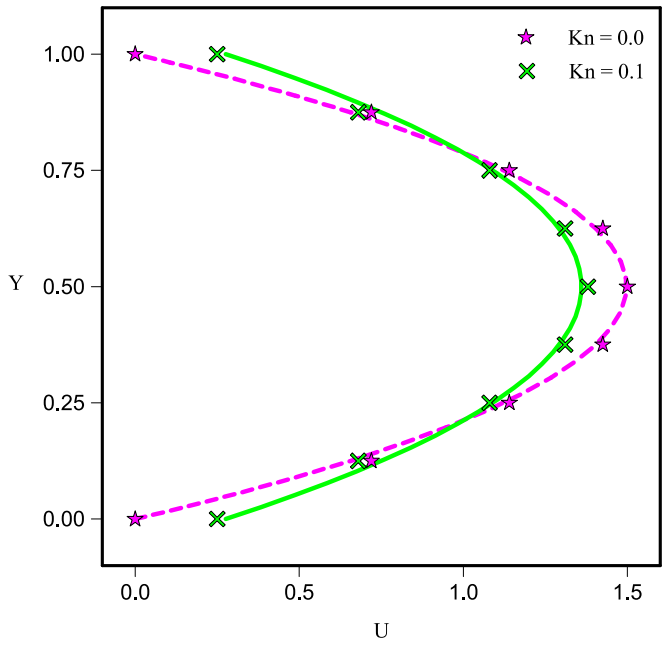

Fig. 2. Fully developed velocity profiles from the present work versus Hooman and Ejlali [61] (Symbols: Hooman and Ejlali [61], Lines: Present work).

$$\rho_{nf} = \varphi\rho_s + (1-\varphi)\rho_f \tag{5}$$

$$\mu_{nf} = \mu_f/(1-\varphi)^{2.5} \tag{6}$$

Moreover Xuan and Li [56] equation is used for the nanofluid heat capacity:

$$(\rho c_p)_{nf} = (1-\varphi)(\rho c_p)_f + \varphi(\rho c_p)_s \tag{7}$$

Nanofluid thermal conductivity can be achieved from Chon et al. formula [57] which is able to consider the nanoparticles diameter and their Brownian motions as follows:

$$\frac{k_{nf}}{k_f} = 1 + 64.7\times\varphi^{0.7460}\left(\frac{d_f}{d_p}\right)^{0.3690}\left(\frac{k_s}{k_f}\right)^{0.7476}\left(\frac{\mu}{\rho_f\alpha_f}\right)^{0.9955}\left(\frac{\rho_f B_c T}{3\pi\mu^2 l_{BF}}\right)^{1.2321} \tag{8}$$

It should be mentioned that l_{BF} in Eq. (8), shows the base fluid mean free path, B_c=1.3807×10^{-23} J/K, represents the Boltzmann constant and μ would be equals to:

$$\mu = A\left(10^{\frac{B}{T-C}}\right),\quad C = 140\ (\mathrm{K}),\quad B = 247\ (\mathrm{K}),\quad A = 2.414(10^{-5})\ (\mathrm{Pa\ s}) \tag{9}$$

Eq. (10) can be used to determine the electrical conductivity of nanofluid according to the electrical conductivity of the base fluid and nanoparticles as follows [55,58]:

$$\frac{\sigma_{nf}}{\sigma_f} = 1 + \frac{3(\sigma_s/\sigma_f - 1)\varphi}{(\sigma_s/\sigma_f + 2) - (\sigma_s/\sigma_f - 1)\varphi} \tag{10}$$

To show the governing equations in non-dimensional form, the following parameters are introduced:

$$\begin{aligned} &H = h/h,\quad L = l/h\\ &Y = y/h,\quad X = x/h\\ &V = v/u_i,\quad U = u/u_i\\ &\theta = (T-T_C)/(T_H-T_C)\\ &P = p/(\rho_{nf}u_i^2) \end{aligned} \tag{11}$$

As a result, the non-dimensional form of the governing Navier-Stokes equations can be derived as:

$$\frac{\partial U}{\partial X} + \frac{\partial V}{\partial Y} = 0 \tag{12}$$

$$U\frac{\partial U}{\partial X} + V\frac{\partial U}{\partial Y} = -\frac{\partial P}{\partial X} + \frac{1}{\mathrm{Re}}\left(\frac{\partial^2 U}{\partial X^2} + \frac{\partial^2 U}{\partial Y^2}\right) - \frac{Ha^2}{\mathrm{Re}}U \tag{13}$$

$$U\frac{\partial V}{\partial X} + V\frac{\partial V}{\partial Y} = -\frac{\partial P}{\partial Y} + \frac{1}{\mathrm{Re}}\left(\frac{\partial^2 V}{\partial X^2} + \frac{\partial^2 V}{\partial Y^2}\right) \tag{14}$$

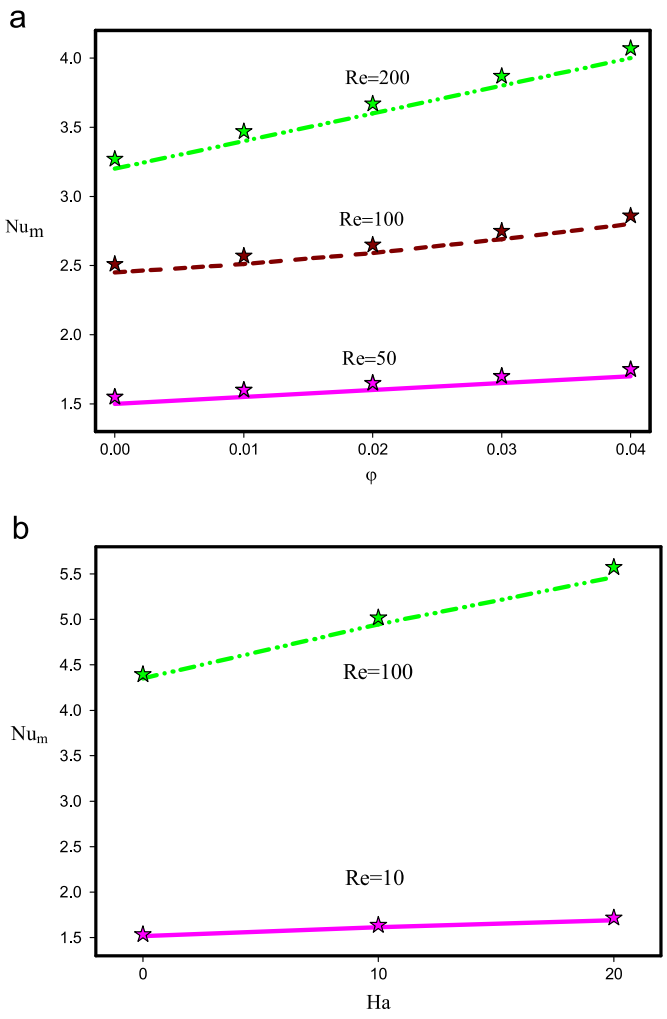

Fig. 3. (a) Nu_m from this article in comparison with Santra et al. [19] (Symbols: Santra et al. [19], Lines: Present work). (b) Nu_m from this article in comparison with Aminossadati et al. [54] at φ=0.02 (Symbols: Aminossadati et al. [54], Lines: Present work).

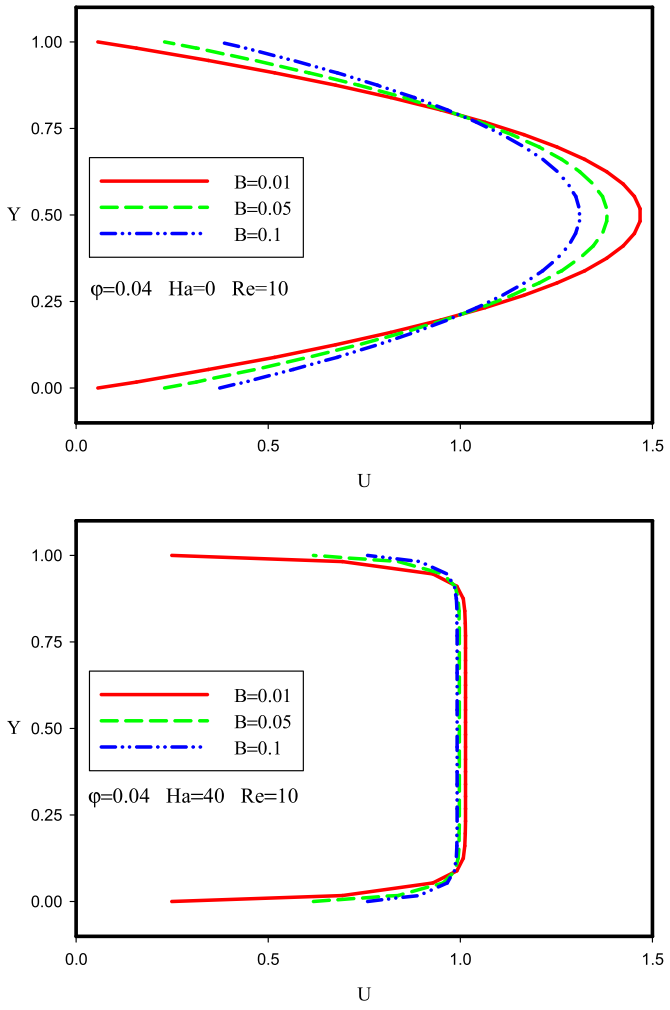

Fig. 4. Fully developed horizontal velocity profiles of U for water-Al_2O_3 nanofluid at φ=0.04, *Re*=10, *Ha*=0 and *Ha*=40 for different values of B.

$$U\frac{\partial\theta}{\partial X}+V\frac{\partial\theta}{\partial Y}=\frac{1}{\mathrm{Re\,Pr}}\left(\frac{\partial^2\theta}{\partial X^2}+\frac{\partial^2\theta}{\partial Y^2}\right) \tag{15}$$

Notes that Reynolds number, Prandtl number and Hartmann number are defined based on the nanofluid properties as $Re=u_i h/\upsilon_{nf}$, $Pr=\upsilon_{nf}/\alpha_{nf}$ and $Ha=B_0 h(\sigma_{nf}/\mu_{nf})^{0.5}$.

4. Boundary conditions

Hot uniform flow is supposed for the inlet as $U_{inlet}=u_i/u_i=1$ and $\theta_{inlet}=1$; while the fully developed condition is achieved at the outlet.

At present study, it is tried to simulate the slip velocity and temperature jump boundary conditions along the microchannel walls. Eq. (16) represents the slip velocity according to the slip length (L_s) [59]:

$$\Delta u_{wall}=u_{fluid}(y\to wall)-u_{wall}=L_s\frac{\partial u_{fluid}(y)}{\partial y}\bigg|_{wall} \tag{16}$$

where u_{wall} and u_{fluid} are the velocity of wall and the velocity of fluid on the wall, respectively. Finally, the slip velocity of nanofluid along the microchannel walls can be determined by using the slip coefficient, β, as follows [60]:

$$u_s=\pm\beta\frac{\partial u}{\partial y}\bigg|_{y=0,h} \tag{17}$$

Eq. (18) shows the non-dimensional slip velocity using B=β/h, as the non-dimensional form of slip coefficient:

$$U_s=\pm B\frac{\partial U}{\partial Y}\bigg|_{Y=0,1} \tag{18}$$

Through the same procedure of developing the slip velocity equation and by using ζ, as the temperature jump distance; Temperature jump values can be determined along the microchannel walls:

$$\Delta T_{wall}=T_{fluid}(y\to wall)-T_{wall}=\zeta\frac{\partial T_{fluid}(y)}{\partial y}\bigg|_{wall} \tag{19}$$

$$\theta_s=\frac{B}{\mathrm{Pr}}\frac{\partial\theta}{\partial Y}\bigg|_{Y=0,1} \tag{20}$$

Moreover the local and averaged nanofluid Nusselt numbers along the microchannel walls are presented as:

$$Nu_X=-\frac{k_{nf}}{k_f}\left(\frac{\partial\theta}{\partial Y}\right)_{Y=0\ (\text{or } Y=1)} \tag{21}$$

$$Nu_m=\frac{1}{L}\int_0^L Nu_X\,dX \tag{22}$$

5. Numerical procedure, grid independency and validation

Finite volume method based on SIMPLE algorithm is used to descritize and solve the governing equations. To do this, an implicit **FORTRAN** computer code is developed to simulate the nanofluid flow and heat transfer. Table 1 shows the thermo-physical properties of different nanoparticles and water.

The values of U and θ at X=L/2 and Y=H/2 for φ=0.04, *Re*=10, *Ha*=0 and B=0.1 and for water-Al_2O_3 nanofluid at different grid nodes are presented in Table 2. Difference between the results of 450×30 and 525×35 are found negligible; so the grid of 450×30 is chosen for the next calculations.

Fully developed velocity profiles from the present work versus Hooman and Ejlali [61] are compared in Fig. 2 at Kn=0 and Kn=0.1. In their work the theoretical results of fully developed hydrodynamic and thermal forced convection in both parallel plate and circular microchannel including slip velocity and temperature jump were studied for flow of both gases and liquids.

More validation which concerns the copper–water nanofluid through two isothermally heated parallel plates is presented in Fig. 3a versus those of Santra et al. [19] for different values of *Re* and φ. Moreover Fig. 3b shows the last validation of forced convection nanofluid flow in a microchannel in the absence of slip velocity and in the presence of magnetic field reported by Aminossadati et al. [54] at *Re*=10, 100 and *Ha*=0, 10, 20. Good agreements between the averaged Nusselt number from the present computer code with those of Santra et al. [19] and Aminossadati et al. [54] in Fig. 3a and b are observed.

6. Results

The laminar forced convection of nanofluid flow in a microchannel is studied numerically. Microchannel domain is under the influence of a magnetic field with the strength of B_0 (Fig. 1). Fig. 4 shows the fully developed horizontal velocity profiles of U for water-Al_2O_3 nanofluid at φ=0.04, *Re*=10, *Ha*=0 and *Ha*=40 for different values of B. Slip coefficient (B) has the significant effects on U profiles from B=0.01 to B=0.1. It is seen that more B corresponds to more slip velocity at Y=0 and Y=1 and less U_{max} at Y=0.5 for *Ha*=0. At the state of *Ha*=40, the Magnetic field makes the Lorentz force in opposite direction of fluid flow. Hence larger *Ha* leads to smaller U_{max} at Y=0.5; and also generates a core of uniform flow from Y≈0.15 to Y≈0.85 which means

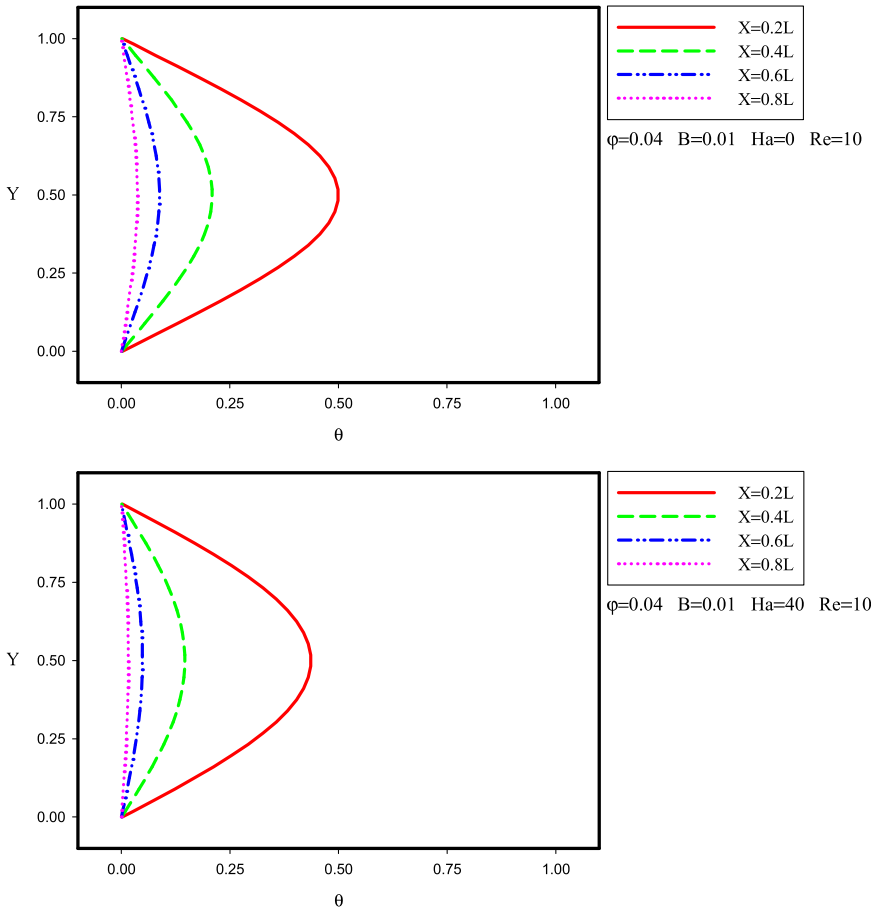

Fig. 5. Temperature profiles of θ at different cross sections of microchannel for water-Al_2O_3 nanofluid at φ=0.04, *Re*=10, B=0.01 for *Ha*=0 and *Ha*=40.

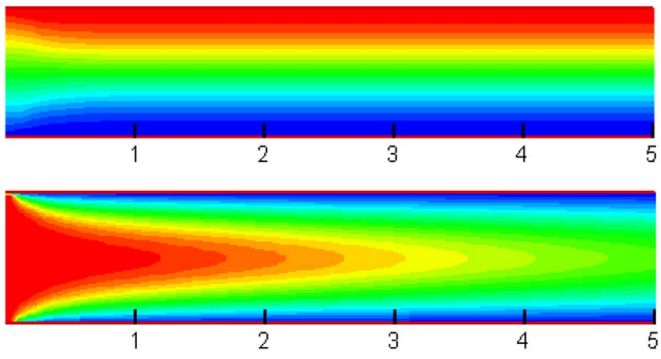

Fig. 6. Streamlines and isotherms of water-Al_2O_3 nanofluid at φ=0.04, B=0.01, *Ha*=0 and *Re*=10.

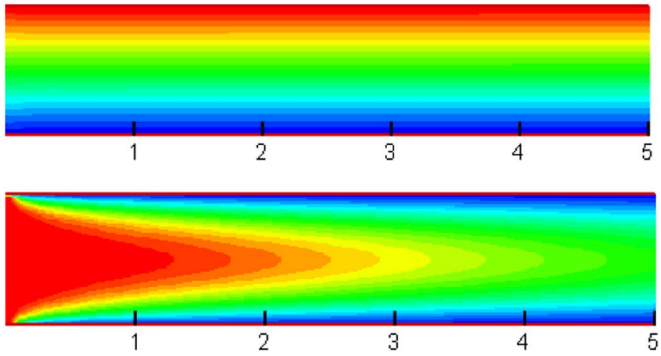

Fig. 7. Streamlines and isotherms of water-Al_2O_3 nanofluid at φ=0.04, B=0.01, *Ha*=40 and *Re*=10.

have the larger fluid velocity adjacent to the walls. However the velocity of this core is not affected significantly by B at higher vales of *Ha*. This fact occurs reversely for slip velocities at Y=0 and Y=1; so that the increase of slip velocity with B would happen more severely at larger *Ha*.

Temperature profiles of θ at different cross sections of microchannel for water-Al_2O_3 nanofluid at φ=0.04, *Re*=10, B=0.01 for *Ha*=0 and *Ha*=40 are observed in Fig. 5. The hot inlet nanofluid is cooled by the heat exchange with the cold microchannel walls through the microchannel so that at X=0.8 L the nanofluid temperature would be almost equal to the walls temperature. Variations of Hartmann number do not have an important effect on θ profiles; however a little reduction could be traced in θ_{max} at Y=0.5 for *Ha*=40 in comparison with the state of *Ha*=0.

To have a better visual aspect of nanofluid flow along the microchannel length, the streamlines and isotherms of water-Al_2O_3 nanofluid at φ=0.04, B=0.01, *Ha*=0 and *Re*=10 are presented in Fig. 6. It should be mentioned that only the region around the entrance length, $0 < X < 5$, are shown in this figure for more clarity. Streamlines are uniform and parallel except through a small space at entrance ($0 < X < 0.5$). Reduce the temperature of hot inlet flow due to heat exchange with the cold walls is well obvious in the isotherms plots of this figure. In order to investigate the effects of magnetic field on the streamlines and isotherm, these contours are drawn in Fig. 7 for *Ha*=40 at φ=0.04, B=0.01 and *Re*=10. The imbalance of streamlines at $0 < X < 0.5$, vanish at the state of *Ha*=40 compared with *Ha*=0 while isotherms plots do not show the sensible change with *Ha*.

One of the most important properties of a micro-flow is slip velocity boundary condition which means the fluid adjacent to the wall does not have the same velocity and is able to slip along it. This phenomenon can be observed clearly in Fig. 8a which concerns the slip velocity

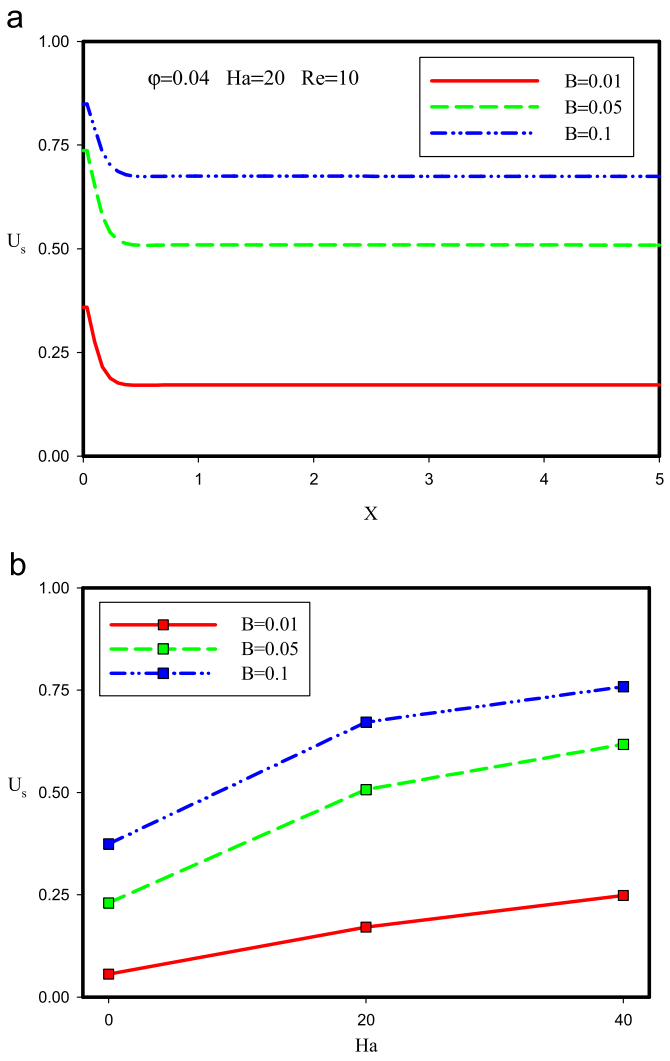

Fig. 8. (a) Slip velocity profiles for water-Al_2O_3 nanofluid along the microchannel wall for different values of B. (b) Slip velocity for water-Al_2O_3 nanofluid versus of *Ha* for different values of B at fully developed condition.

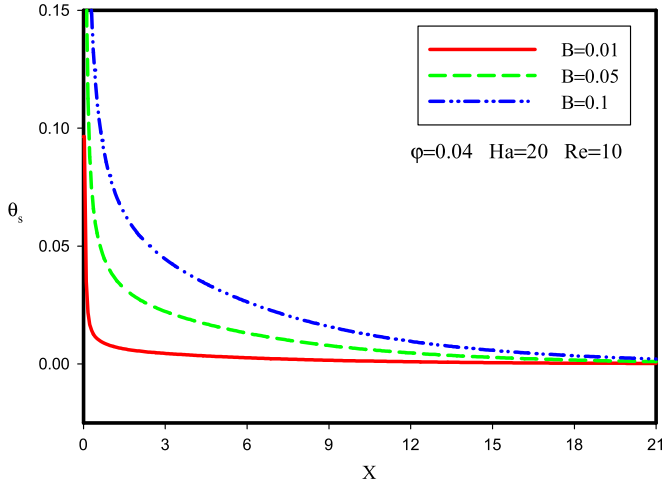

Fig. 9. Temperature jump for water-Al_2O_3 nanofluid along the microchannel wall for φ=0.04, *Re*=10 and *Ha*=20 at different values of B.

profiles for water-Al_2O_3 nanofluid along the microchannel wall for different values of B at φ=0.04, *Re*=10 and *Ha*=20. Slip velocity profile begins from its greatest amount at entrance and then it reduces along the microchannel wall so that tends to the specified value. This figure

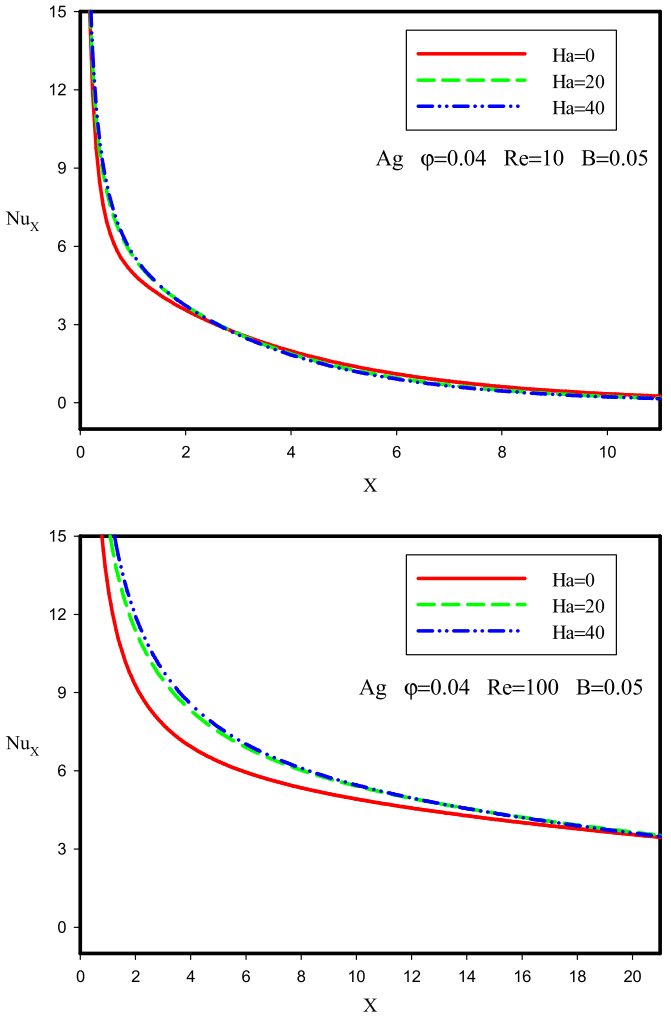

Fig. 10. Nu_X for water-Ag nanofluid along the microchannel wall at different values of *Ha* and *Re* for φ=0.04 and B=0.05.

implies the significant effect of B on U_s.

The effects of *Ha* on slip velocity can be studied in Fig. 8b; where such this research case has not been reported before in the literature. It is observed that the positive effects of slip coefficient on the slip velocity can be occurred more severely at higher Hartmann numbers; which means stronger magnetic field invigorates the micro-scale properties. As a result, the highest value of slip velocity at fully developed condition is achieved at highest amounts of slip coefficient and Hartmann number as B=0.1 and *Ha*=40.

Temperature jump variations along the microchannel wall are presented in Fig. 9 for water-Al_2O_3 nanofluid at φ=0.04, *Re*=10, *Ha*=20 and different values of B. Temperature jump effects are ignored in the most previous articles; however Fig. 9 implies that its values are sensible at $0 < X < 15$ and should be involved especially at microchannel entrance space where has the most heat exchange with the walls. Larger B corresponds to larger θ_s, while the effects of *Ha* can be ignored on.

Local profiles of Nusselt number for water-Ag nanofluid along the microchannel wall at different values of *Ha* and *Re* for φ=0.04 and B=0.05 are shown in Fig. 10. Nu_X begins from its greatest amount at inlet and then decreases along the microchannel wall.

To better explain the heat transfer rate from the walls, the averaged Nusselt numbers at different values of *Ha* and B for *Re*=10 and *Re*=100 at φ=0.04 are presented in Fig. 11. At higher values of *Re* as *Re*=100, Nu_m of Ag-water nanofluid is larger than Al_2O_3-water one. This well known fact is because of the higher thermal conductivity of Ag;

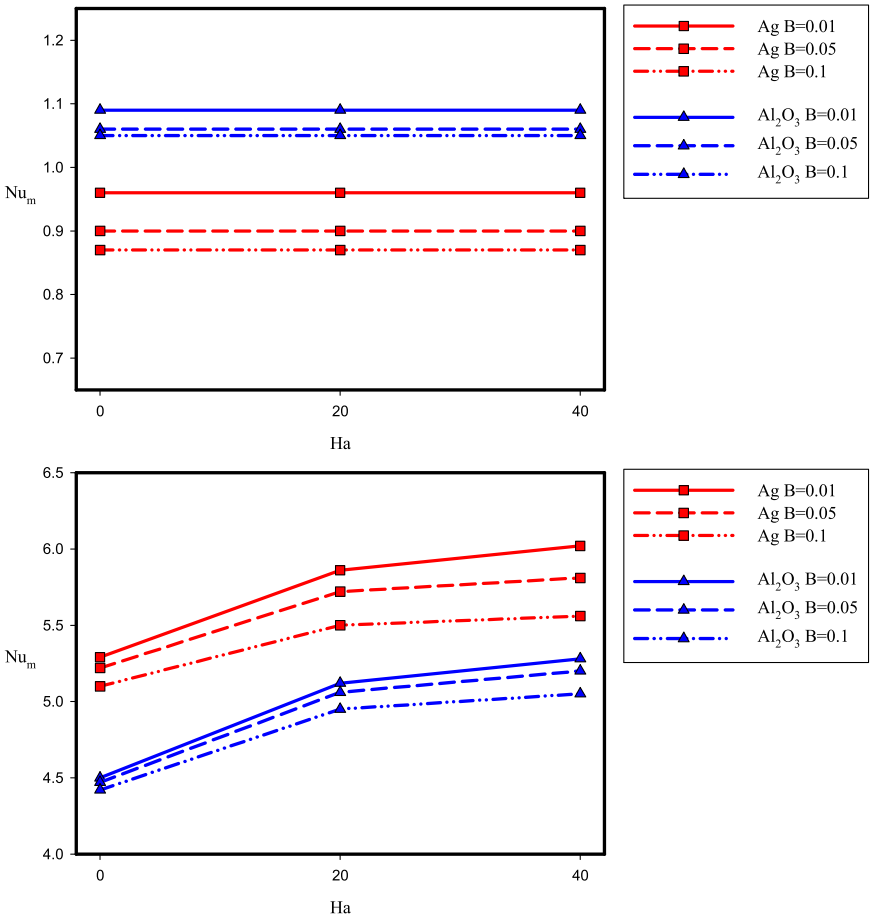

Fig. 11. Nu_m on the microchannel wall at different values of *Ha* and B for *Re*=10 (top) and *Re*=100 (bottom) at φ=0.04.

however at lower values of *Re* as *Re*=10, this procedure occurs reversely. As it is said before the nanofluid Reynolds number through a microchannel usually has a small value to illustrate the real physical situation. As a result and in order to increase the heat transfer rate from a real microchannel (at low *Re*), it is proposed to use the Al_2O_3-water nanofluid instead of Ag-water. However at larger values of *Re* (as *Re*=100) the nanofluid composed of nanoparticles with higher thermal conductivity would work better.

Showing the roll of slip coefficient on Nu_m could be another interesting point of Fig. 11. More B corresponds to less Nu_m; which means averaged Nusselt number decreases due to slip velocity boundary condition. The reader approaches to a new finding with more focus on Fig. 11. It is seen that larger *Ha* leads to larger Nu_m at higher values of *Re* (as *Re*=100); so the stronger magnetic field increases the heat transfer rate however this phenomenon is not significant at low values of Reynolds number.

7. Conclusion

Forced convection of nanofluid (Ag-water and Al_2O_3-water) flow in a microchannel was studied numerically. Microchannel domain was under the influence of a magnetic field. The investigation of magnetic field effect on slip velocity and temperature jump was presented for the first time and the following points were obtained:

Magnetic field makes the Lorentz force in opposite direction of fluid flow; Hence larger Hartmann number (*Ha*) leads to smaller U_{max} at Y=0.5 and also generates a core of uniform flow from Y≈0.15 to Y≈0.85. Moreover larger *Ha* leads to larger Nu_m, at higher values of *Re*.

More slip coefficient (B) corresponds to less Nu_m and more U_s, especially at larger *Ha*. The highest value of U_s, at fully developed condition is achieved at highest amounts of B and *Ha* as B=0.1 and *Ha*=40.

Temperature jump (θ_s) effects should be involved at microchannel entrance area where the most heat exchange with the walls happen. Larger B corresponds to larger θ_s, while the effects of *Ha* can be ignored on.

It is recommended to use Al_2O_3-water nanofluid instead of Ag-water to increase the heat transfer rate from the microchannel walls at low values of *Re*. However at larger amounts of *Re*, the nanofluid composed of nanoparticles with higher thermal conductivity works better.

References

[1] S. Lee, S.U.S. Choi, S. Li, J.A. Eastman, Measuring thermal conductivity of fluids containing oxide nanoparticles, ASME J. Heat Transf. 121 (1999) 280–289.
[2] M.H. Esfe, S.S.M. Esforjani, M. Akbari, A. Karimipour, Mixed-convection flow in a lid driven square cavity filled with a nanofluid with variable properties: effect of the nanoparticle diameter and of the position of a hot obstacle, Heat Transf. Res. 45 (2014) 563–578.
[3] N.S. Akbar, Ferromagnetic CNT suspended H_2O+Cu nanofluid analysis through composite stenosed arteries with permeable wall, Physica E: Low-Dimens. Syst. Nanostruct. 72 (2015) 70–76.
[4] M.H. Esfe, S. Saedodin, M. Akbari, A. Karimipour, M. Afrand, S. Wongwises, M.R. Safaei, M. Dahari, Experimental investigation and development of new correlations for thermal conductivity of CuO/EG–water nanofluid, Int. Commun. Heat Mass Transf. 65 (2015) 47–51.
[5] M.H. Esfe, A. Naderi, M. Akbari, M. Afrand, A. Karimipour, Evaluation of thermal conductivity of COOH-functionalized MWCNTs/water via temperature and solid volume fraction by using experimental data and ANN methods, J. Therm. Anal. Calorim. 121 (3) (2015) 1273–1278.
[6] N.S. Akbar, Biofluidics study in digestive system with thermal conductivity of shape nanosize H_2O+Cu nanoparticles, J. Bionic Eng. 12 (4) (2015) 656–663.
[7] M.H. Esfe, A.A.A. Arani, A. Karimipour, S.S.M. Esforjani, Numerical simulation of natural convection around an obstacle placed in an enclosure filled with different

types of nanofluids, Heat Transf. Res. 45 (2014) 279–292.
[8] N.S. Akbar, Z.H. Khan, Effect of variable thermal conductivity and thermal radiation with CNTS suspended nanofluid over a stretching sheet with convective slip boundary conditions: numerical study, J. Mol. Liq. 222 (2016) 279–286.
[9] M. Baratpour, A. Karimipour, M. Afrand, S. Wongwises, Effects of temperature and concentration on the viscosity of nanofluids made of single-wall carbon nanotubes in ethylene glycol, Int. Commun. Heat Mass Transf. 74 (2016) 108–113.
[10] N.S. Akbar, A new thermal conductivity model with shaped factor ferromagnetism nanoparticles study for the blood flow in non-tapered stenosed arteries, IEEE Trans. Nanobiosci. 14 (7) (2015) 780–789.
[11] N.S. Akbar, M.T. Mustafa, Ferromagnetic effects for nanofluid venture through composite permeable stenosed arteries with different nanosize particles, AIP Adv. 5 (7) (2015) 077102.
[12] M.H. Esfe, S. Saedodin, A. Asadi, A. Karimipour, Thermal conductivity and viscosity of Mg (OH) 2-ethylene glycol nanofluids, J. Therm. Anal. Calorim. 120 (2) (2015) 1145–1149.
[13] H.F. Oztop, E. Abu-Nada, Numerical study of natural convection in partially heated rectangular enclosures filled with nanofluids, Int. J. Heat Fluid Flow 29 (2008) 1326–1336.
[14] R.K. Tiwari, M.K. Das, Heat transfer augmentation in a two-sided lid-driven differentially heated square cavity utilizing nanofluid, Int. J. Heat Mass Transf. 50 (2007) 2002–2018.
[15] N.S. Akbar, M. Raza, R. Ellahi, Copper oxide nanoparticles analysis with water as base fluid for peristaltic flow in permeable tube with heat transfer, Comput. Methods Prog. Biomed. 130 (2016) 22–30.
[16] A. Karimipour, A.H. Nezhad, A. Behzadmehr, S. Alikhani, E. Abedini, Periodic mixed convection of a nanofluid in a cavity with top lid sinusoidal motion, Proc. IMechE Part C: J. Mech. Eng. Sci. 225 (2011) 2149–2160.
[17] A. Karimipour, M.H. Esfe, M.R. Safaei, D.T. Semiromi, S.N. Kazi, Mixed convection of copper–water nanofluid in a shallow inclined lid driven cavity using the lattice Boltzmann method, Physica A 402 (2014) 150–168.
[18] M.H. Esfe, M. Akbari, D. Toghraie, A. Karimipour, M. Afrand, Effect of nanofluid variable properties on mixed convection flow and heat transfer in an inclined two-sided lid-driven cavity with sinusoidal heating on sidewalls, Heat Transf. Res. 45 (2014) 409–432.
[19] A.K. Santra, S. Sen, N. Chakraborty, Study of heat transfer due to laminar flow of copper–water nanofluid through two isothermally heated parallel plates, Int. J. Therm. Sci. 48 (2009) 391–400.
[20] M.H. Esfe, M. Akbari, A. Karimipour, M. Afrand, O. Mahian, S. Wongwises, Mixed-convection flow and heat transfer in an inclined cavity equipped to a hot obstacle using nanofluids considering temperature-dependent properties, Int. J. Heat Mass Transf. 85 (2015) 656–666.
[21] A. Karimipour, M. Afrand, M. Akbari, M.R. Safaei, Simulation of fluid flow and heat transfer in the inclined enclosure, World Acad. Sci. Eng. Technol. 61 (2012) 435–440.
[22] M.R. Safaei, O. Mahian, F. Garoosi, K. Hooman, A. Karimipour, S.N. Kazi, S. Gharehkhani, Investigation of micro- and nanosized particle erosion in a 90° pipe bend using a two-phase discrete phase model, Sci. World J. (2014). http://dx.doi.org/10.1155/2014/740578 12 pp..
[23] A. Behzadmehr, M. Saffar-Avval, N. Galanis, Prediction of turbulent forced convection of a nanofluid in a tube with uniform heat flux using a two phase approach, Int. J. Heat Fluid Flow 28 (2007) 211–219.
[24] C. Abdellahoum, A. Mataoui, H.F. Oztop, Turbulent forced convection of nanofluid over a heated shallow cavity in a duct, Powder Technol. 277 (2015) 126–134.
[25] M. Gad-el-Hak, Flow physics in MEMS, Rev Mec. Ind. 2 (2001) 313–341.
[26] H.P. Kavehpour, M. Faghri, Y. Asako, Effects of compressibility and rarefaction on gaseous flows in microchannels, Numer. Heat Transf. Part A 32 (1997) 677–696.
[27] M. Goodarzi, M.R. Safaei, H.F. Oztop, A. Karimipour, E. Sadeghinezhad, M. Dahari, S.N. Kazi, N. Jomhari, Numerical study of entropy generation due to coupled laminar and turbulent mixed convection and thermal radiation in an enclosure filled with a semitransparent medium, Sci. World J. (2014). http://dx.doi.org/10.1155/2014/761745 8 pp..
[28] N.T. Nguyen, S.T. Wereley, Fundamentals and Applications of Microfluidics, second edition, Artech House Inc., Norwood, MA, 2006.
[29] M. El Abdallaoui, M. Hasnaoui, A. Amahmid, Numerical simulation of natural convection between a decentered triangular heating cylinder and a square outer cylinder filled with a pure fluid or a nanofluid using the lattice Boltzmann method, Powder Technol. 277 (2015) 193–205.
[30] A. Raisi, B. Ghasemi, S.M. Aminossadati, A numerical study on the forced convection of laminar nanofluid in a microchannel with both slip and no-slip conditions, Numeric, Heat Transf. Part A 59 (2011) 114–129.
[31] M. Mital, Analytical analysis of heat transfer and pumping power of laminar nanofluid developing flow in microchannels, Appl. Therm. Eng. 50 (2013) 429–436.
[32] M. Nojoomizadeh, A. Karimipour, The effects of porosity and permeability on fluid flow and heat transfer of multi walled carbon nano-tubes suspended in oil (MWCNT/Oil nano-fluid) in a microchannel filled with a porous medium, Physica E: Low-Dimens. Syst. Nanostruct. (2016).
[33] W.H. Mah, Y.M. Hung, N. Guo, Entropy generation of viscous dissipative nanofluid flow in microchannels, Int. J. Heat Mass Transf. 55 (2012) 4169–4182.
[34] M. Kalteh, A. Abbassi, M. Saffar-Avval, J. Harting, Eulerian–Eulerian two-phase numerical simulation of nanofluid laminar forced convection in a microchannel, Int. J. Heat Fluid Flow 32 (2011) 107–116.
[35] A. Karimipour, New correlation for Nusselt number of nanofluid with Ag/Al2O3/Cu nanoparticles in a microchannel considering slip velocity and temperature jump by using lattice Boltzmann method, Int. J. Therm. Sci. 91 (2015) 146–156.
[36] Y. Xuan, Q. Li, M. Ye, Investigations of convective heat transfer in ferrofluid microflows using lattice-Boltzmann approach, Int. J. Therm. Sci. 46 (2007) 105–111.
[37] X. Nie, G.D. Doolen, S. Chen, Lattice-Boltzmann simulation of fluid flows in MEMS, J. Stat. Phys. 107 (2002) 279–289.
[38] M. Goodarzi, M.R. Safaei, A. Karimipour, K. Hooman, M. Dahari, S.N. Kazi, E. Sadeghinezhad, Comparison of the finite volume and Lattice Boltzmann methods for solving natural convection heat transfer problems inside cavities and enclosures, Abstr. Appl. Anal. (2014). http://dx.doi.org/10.1155/2014/762184 15 pp..
[39] A. Karimipour, A.H. Nezhad, A. D'Orazio, E. Shirani, The effects of inclination angle and Prandtl number on the mixed convection in the inclined lid driven cavity using lattice Boltzmann method, J. Theor. Appl. Mech. 51 (2013) 447–462.
[40] A. Karimipour, A.H. Nezhad, A. D'Orazio, E. Shirani, Investigation of the gravity effects on the mixed convection heat transfer in a microchannel using lattice Boltzmann method, Int. J. Therm. Sci. 54 (2012) 142–152.
[41] G.Bird, Molecular Gas Dynamics and the Direct Simulation of Gas Flows, Oxford, 1994.
[42] A. Karimipour, A.H. Nezhad, E. Shirani, A. Safaei, Simulation of fluid flow and heat transfer in inclined cavity using Lattice Boltzmann method, World Acad. Sci. Eng. Technol. 5 (2011) 558–565.
[43] F. Hedayati, G. Domairry, Effects of nanoparticle migration and asymmetric heating on mixed convection of TiO_2–H_2O nanofluid inside a vertical microchannel, Powder Technol. 272 (2015) 250–259.
[44] A. Malvandi, D.D. Ganji, Mixed convective heat transfer of water/alumina nanofluid inside a vertical microchannel, Powder Technol. 263 (2014) 37–44.
[45] A. Mahmoudi, I. Mejri, M.A. Abbassi, A. Omri, Lattice Boltzmann simulation of MHD natural convection in a nanofluid-filled cavity with linear temperature distribution, Powder Technol. 256 (2014) 257–271.
[46] F. Hedayati, A. Malvandi, M.H. Kaffash, D.D. Ganji, Fully developed forced convection of alumina/water nanofluid inside microchannels with asymmetric heating, Powder Technol. 269 (2015) 520–531.
[47] A. Karimipour, A.H. Nezhad, A. D'Orazio, M.H. Esfe, M.R. Safaei, E. Shirani, Simulation of copper–water nanofluid in a microchannel in slip flow regime using the lattice Boltzmann method, Eur. J. Mech. B/Fluids 49 (2015) 89–99.
[48] R. Ellahi, The effects of MHD and temperature dependent viscosity on the flow of non-Newtonian nanofluid in a pipe: analytical solutions, Appl. Math. Model. 37 (2013) 1451–1467.
[49] R.U. Haq, S. Nadeem, Z.H. Khan, N.S. Akbar, Thermal radiation and slip effects on MHD stagnation point flow of nanofluid over a stretching sheet, Physica E: Low-Dimens. Syst. Nanostruct. 65 (2015) 17–23.
[50] M. Mahmoodi, M.H. Esfe, M. Akbari, A. Karimipour, M. Afrand, Magneto-natural convection in square cavities with a source-sink pair on different walls, Int. J. Appl. Electromagn. Mech. 47 (2015) 21–32.
[51] P. Forghani-Tehrani, A. Karimipour, M. Afrand, S. Mousavi, Different nano particles volume fraction and Hartmann number effects on flow and heat transfer of water-silver nanofluid under the variable heat flux, Physica E: Low-Dimens. Syst. Nanostruct. (2016).
[52] A. Malvandi, D.D. Ganji, Effects of nanoparticle migration and asymmetric heating on magnetohydrodynamic forced convection of alumina/water nanofluid in microchannels, Eur. J. Mech. – B/Fluids 52 (2015) 169–184.
[53] N. Hajialigol, A. Fattahi, M. Haji Ahmadi, M. Ebrahim Qomi, E. Kakoli, MHD mixed convection and entropy generation in a 3-D microchannel using Al_2O_3–water nanofluid, J. Taiwan Inst. Chem. Eng. 46 (2015) 30–42.
[54] S.M. Aminossadati, A. Raisi, B. Ghasemi, Effects of magnetic field on nanofluid forced convection in a partially heated microchannel, Int. J. Non-Linear Mech. 46 (2011) 1373–1382.
[55] A.H. Mahmoudi, I. Pop, M. Shahi, Effect of magnetic field on natural convection in a triangular enclosure filled with nanofluid, Int. J. Therm. Sci. 59 (2012) 126–140.
[56] Y. Xuan, Q. Li, Investigation on convective heat transfer and flow features of nanofluids, ASME J. Heat Transf. 125 (2003) 151–155.
[57] C.H. Chon, K.D. Kihm, S.P. Lee, S.U.S. Choi, Empirical correlation finding the role of temperature and particle size for nanofluid (AL_2O_3) thermal conductivity enhancement, Appl. Phys. Lett. 87 (2005) 1–3.
[58] J.C. Maxwell, A Treatise on Electricity and Magnetism, second edition, Oxford University Press, Cambridge, 1904, pp. 435–441.
[59] P.A. Thompson, S.M. Troian, A general boundary condition for liquid flow at solid surfaces, Phys. Rev. Lett. 63 (1997) 766–769.
[60] G.D. Ngoma, F. Erchiqui, Heat flux and slip effects on liquid flow in a microchannel, Int. J. Therm. Sci. 46 (2007) 1076–1083.
[61] K. Hooman, A. Ejlali, Effects of viscous heating, fluid property variation, velocity slip, and temperature jump on convection through parallel plate and circular microchannels, Int. Commun. Heat Mass Transf. 37 (1) (2010) 34–38.